chemistry proceedings

MDPI

Proceeding Paper

Effect of Oxygen on the Optical Properties of Citric Acid-Based Carbon Dots †

Federico Turco, Benedetta Maria Squeo, Francesca Villafiorita Monteleone, Chiara Botta and Mariacecilia Pasini *

Institute of Chemical Sciences and Technologies (SCITEC)—CNR, 20133 Milano, Italy; federico.turco@scitec.cnr.it (F.T.); benedetta.squeo@scitec.cnr.it (B.M.S.); francesca.villafiorita@scitec.cnr.it (F.V.M.); chiara.botta@scitec.cnr.it (C.B.)

* Correspondence: mariacecilia.pasini@scitec.cnr.it

† Presented at The 28th International Electronic Conference on Synthetic Organic Chemistry (ECSOC 2024), 15–30 November 2024; Available online: https://sciforum.net/event/ecsoc-28.

Abstract: In this contribute the photophysical properties of CDs obtained as described in literature from Citric Acid, Formic Acid and Urea were studied in two different solvents, water and DMSO and under nitrogen and oxygen atmosphere. The results indicate a possible doping effect of Oxygen which significantly impacts the optical proprieties.

Keywords: CDs; photophysical properties; Oxygen

1. Introduction

Carbon dots (CDs) are an emerging class of 0-dimensional nanoparticles belonging to the carbon-based family of materials. Characterized by a graphene-like core surrounded by amorphous, functionalized carbon, these nanoparticles are typically less than 20 nm in size and were first reported in 2004 [1]. Over the past few years, CDs have attracted significant attention due to their unique and advantageous properties. They are easily synthesized from a broad range of low-cost starting materials via bottom-up approaches, making their production highly scalable and economically viable [2]. In addition, their biocompatibility, low cytotoxicity [3], tunable photoluminescence [4], and photo-induced electron transfer capabilities have positioned CDs as versatile materials for applications in sensing [5], bio-imaging [6], catalysis [7,8], photodynamic therapy [9,10], packaging [11], and optoelectronic devices [12]. Because of these qualities, CDs are increasingly seen as a promising organic alternative to metal-based quantum dots.

Despite their potential, there remain significant challenges in understanding the correlation between the optical properties of CDs and their nanoparticle structure. Achieving reproducibility in their synthesis and gaining insight into the mechanisms behind their photoluminescence is one of the primary hurdles in fully exploiting the potential of these carbon-based nanoparticles.

In particular, CDs that exhibit efficient excitation and emission in the deep-red [13–15] and near-infrared (NIR) [16,17] spectral ranges are of considerable interest for bioimaging applications. Emission in these regions is crucial for in vivo imaging since tissue autofluorescence and light scattering are minimized, leading to improved imaging contrast and spatial resolution. Several research groups have reported on CDs with deep-red and/or NIR emissions, typically excited by light in the green spectral region. To achieve such emissions, various techniques such as heteroatom doping, size control, surface engineering, and chemical environment modulation of CDs have been explored. For instance, Jiang et al. reported CDs [18] with full-range UV-Vis-NIR emission through fluorine and nitrogen co-doping, where the optimum excitation wavelength was around 550 nm with a photoluminescence quantum yield (PLQY) of 9.8%.

Citation: Turco, F.; Squeo, B.M.; Monteleone, F.V.; Botta, C.; Pasini, M. Effect of Oxygen on the Optical Properties of Citric Acid-Based Carbon Dots. *Chem. Proc.* **2024**, *6*, x. https://doi.org/10.3390/xxxxx

Academic Editor(s): Name

Published: 15 November 2024

Efficient red-emissive CDs in aqueous solutions remain scarce, which limits their performance in high-resolution bioimaging. However, some progress has been made. For example, a one-step solvothermal method has been developed to synthesize pure red-emissive CDs (FA-CDs) [20] from citric acid and urea in formic acid, avoiding the need for complicated purification procedures. Additionally, surface modifications of CDs have been found to affect their NIR absorption and emission properties. The adsorption of electron-acceptor groups on the CD surface can enhance NIR emission, and it has been demonstrated that the deprotonation of surface hydroxyl groups can shift the absorption band toward longer wavelengths while also enhancing emission intensity by inhibiting energy dissipation [19].

Understanding the factors that influence photoluminescence emission and photothermal conversion in the deep-red/NIR regions is of utmost importance for the design of CDs with enhanced emission in these ranges. One major area of study is the role of surface hydroxyl groups, which are commonly found on CDs. The protonation and deprotonation processes at the CD surface significantly impact their energy structure, yet relatively few studies have investigated the effects of surface protonation on these optical properties. Moreover, in applications for in vivo bioimaging, the effect of environmental oxygen on CDs must be carefully considered. Unlike in electronic applications, oxygen is always present in biological systems, and its interaction with CDs could influence their optical behavior.

In light of this, the present study examines the combined effects of solvent and oxygen on the optical properties of CDs. Building on previous work by Zhang et al. [20], which successfully demonstrated the use of CDs for in vivo applications, we analyze how both UV absorption and photoluminescence are affected by oxygen exposure. Our results suggest that oxygen may play a role in doping the CDs, thereby altering their optical properties. Understanding these interactions is critical for the development of CDs that are optimized for biological imaging, where oxygen is an unavoidable component of the environment. This study contributes to the growing body of knowledge regarding the factors that influence the optical behavior of CDs, particularly in biologically relevant conditions.

By continuing to explore the relationship between CD structure, surface chemistry, and optical properties, researchers aim to enhance the reproducibility and efficiency of CDs, bringing us closer to realizing their full potential in a wide range of applications, especially in biomedical imaging and therapy.

2. Materials and Methods

2.1. Materials

Citric Acid was provided by Tokyo Chemicals Industry Co. (Belgium); Urea was provided by J.T. Baker Chemicals (Holland); Hydrazine by Fluka Chemika (Switzerland); Formic Acid, DMSO, Ethanol from Merck (Germany). Omnipore 0.45 μm PTFE filters are provided from Merck; 0.22 μm Nylon syringe filters are provided by Branchia.

2.2. Instruments

The autoclave is a Buchi Tinyclave with Teflon insert in Steel body; Atomic Force Microscopy (AFM) was performed with AFM NTMDT NTEGRA (NT-MDT Spectrum Instruments LLC. Moscow, Russia) in tapping mode with a cantilever NSG10 operating at a typical cantilever resonance frequency of 140–390 kHz, UV-Vis analysis are performed with Perkin Elmer UV/VIS/NIR Lambda 900, Luminescence measurements with NanoLog composed by a iH320 spectrograph equipped with a Synapse QExtra charge-coupled device by exciting with a monochromated 450W Xe lamp, FT-IR characterization with a Bruker Tensor 27. The quartz cuvette used for Abs and Em has a path length of 1 cm and it has a quartz cap with a sink.

2.3. Methods

The CDs have been obtained through solvothermal reaction in autoclave from Citric Acid and Urea using Formic Acid as solvent according to literature [20]. Briefly, 1 g of Citric Acid (5.2 mmol) and 2 g of Urea (6.4 eq) were placed in a 25-mL Teflon-lined autoclave and dissolved in Formic Acid with the aid of magnetic stirring. Once the reagents are solubilized, the autoclave is heated in an oil bath at 160 °C for 4 h. Then the autoclave is cooled down to room temperature and the reaction mixture is diluted with 40 mL of Ethanol, that lead CDs to precipitate. After centrifugation at 6000 rpm for ten minutes; the supernatant solution is removed, and the CDs are redispersed in Ethanol and centrifugated other 2 times to remove unreacted precursors and the blue absorbing fraction of CDs. At the end the washed solid is dissolved in distilled Water and filtered firstly on a 0.45 μm buchner filter and then through a 0.22 μm syringe filter. The solution is dried using rotary evaporator to obtain a black powder.

Absorption and emission spectra have been registered both in Distilled water and DMSO, the solutions are prepared in inert environment under Nitrogen gas, the CDs sample powder have undergone several Nitrogen-vacuum cycles to ensure the absence of Oxygen.

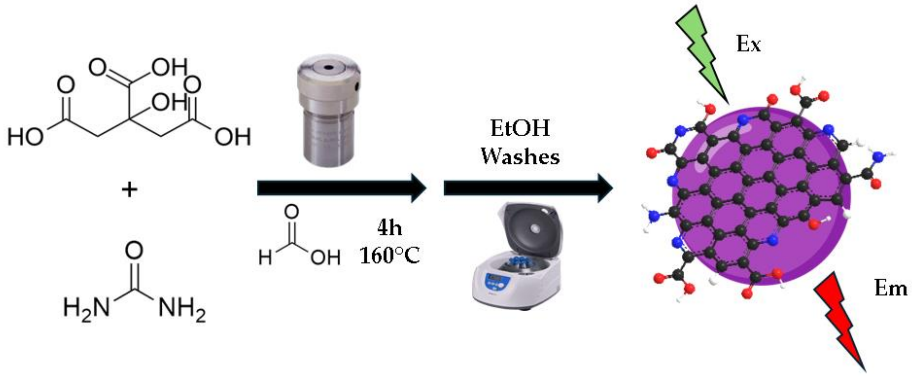

Figure 1. Synthesis scheme of CDots.

3. Results and Discussion

Characterization

The dimensions of the synthetized CDs have been evaluated through AFM technique; the height of the sample is 12–15 nm. The FT-IR shows absorption peaks at 3550 cm^{-1} ν of O-H dimers, 3475 cm^{-1} and 3415 cm^{-1} ν of N-H of primary amides or amines, peak at 2962 cm^{-1} ν of CH_3 and CH_2, peak at 2923 cm^{-1} ν of =C-H, 1704 cm^{-1} ν of C=O, 1627 cm^{-1} and 1618 cm^{-1} of $COO^-/COONH_4$, 1401 cm^{-1} and 1386 cm^{-1} of C-O groups. Elemental analysis reveals the composition of the CDs (C, H, N, O), with the Oxygen value obtained by difference of the others: C (45.63%), H (4.12%), N (14.12%), O (36.13%).

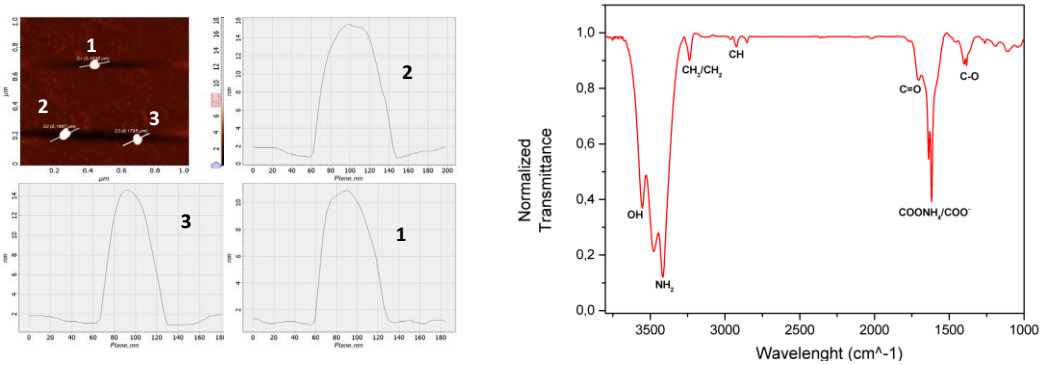

Figure 2. On the left AFM image and particles profile, on the right FT-IR spectrum in KBr.

To verify a possible effect of Oxygen over absorption/emission properties spectra have been recorded for 4 different solutions for each solvent: one solution made with degassed solvent identified as "Solvent + N_2", one "Solvent + O_2" obtained from "Solvent + N_2" after bubbling Oxygen inside identified as "Solvent +O_2 + Hydrazine" obtained from the previous one with the addition of hydrazine, and a fresh one "Solvent + N_2 + Hydrazine".

Hydrazine is reported in the literature as an agent used for the de-doping of organic materials [21,22]. This is particularly relevant in cases of oxygen-induced doping, as oxygen often acts as an electron acceptor in conjugated polymers, leading to an increase in charge carrier concentration, essentially creating a "doped" state. Hydrazine, being a strong reducing agent, has the ability to remove these charge carriers and restore the polymer to its neutral or "de-doped" state. Hydrazine is widely used in the treatment of organic materials because it is compatible with the chemical structure of conjugated polymers. It does not damage the polymer chain but acts selectively on the oxidized groups, preserving the desired electronic properties of the material. Thus, CDs can be seen as analogous to organic conjugated polymers [23,24], both in terms of their structural versatility and the presence of functional groups that define their interactions with light, charge carriers, and other materials for this reason we decide the treatment with hydrazine of the solutions.

In Figure 3 are reported on the left the Absorption and Emission spectra at different excitation wavelength of CDs in water under N_2. The absorption spectrum has a main absorption band at 556 nm and an excitation-dependent PL (photoluminescence) emission In Water (N_2) the overall Luminescence is composed by 3 contributes [25]: one in blue range at about 498 nm, one in the yellow area (598 nm) and one red component at 645 nm. In Figure 3 on the right are reported the absorption spectra in water with and without Oxygen, and after treatment with hydrazine. No significant changes are observed in the absorption positions, but a broadening of the bands and an increased long wavelength tail are noted compared to the corresponding spectra treated with hydrazine.

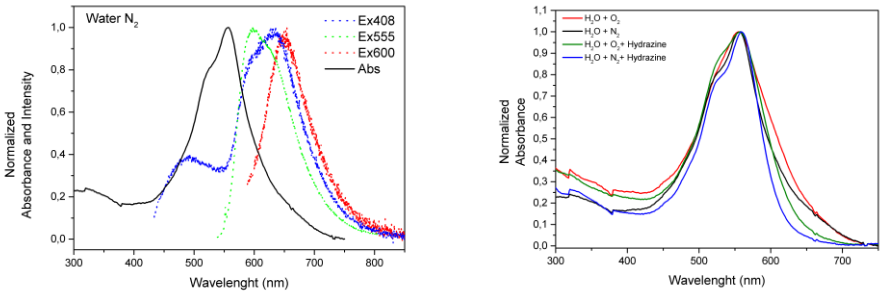

Figure 3. On the left Absorption and Emission (dotted lines) spectra at different excitation wavelength of CDs in H_2O under N_2, on the right Absorption of CDs in H_2O in the 4 conditions.

In Figure 4 are reported on the left the Absorption and Emission spectra at different excitation wavelength of CDs in DMSO under N_2. The absorption spectrum has a main absorption band at 580 nm and two shoulders, one at high energy at about 540 nm and one at lower energy at about 605 nm and a strongly excitation-dependent PL emission. Also, in the DMSO solvent three different emissions can be recognized, a broad one in the blue region, at about 470 nm (τ_{av} = 7.46 ns), and two sharper ones in the yellow and red regions, at 583 nm (τ_{av} = 3.84 ns) and 640 nm (τ_{av} = 2.74 ns), respectively. The different behavior in the two solvents, as previously observed in literature [26], is due to the fact that while water is a polar protic solvent, DMSO is a polar aprotic solvent with good deprotonation ability due to the S = O groups and strong electron-withdrawing ability. It had been demonstrated that deprotonation of the surface can enhance the surface electron-withdrawing environment of CDs, leading to redshifted absorption band, and enhanced

emission intensity by inhibiting the energy dissipation of hydroxyl groups [20]. Indeed, the PL Quantum Yields of water and DMSO solutions, measured under N_2, display values of 15% and 54% for water and DMSO solutions, respectively (see Table 1).

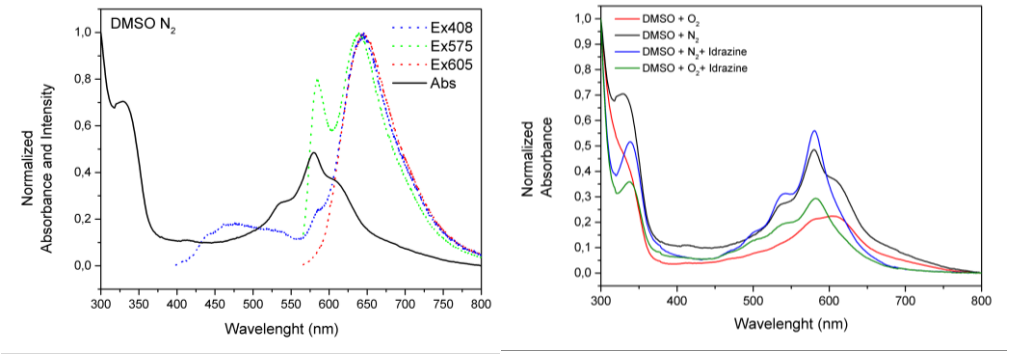

Figure 4. On the left Absorption and Emission spectra at different excitation wavelength of CDs in DMSO solution under N_2, on the right Absorption of CDs in DMSO in the 4 conditions.

Table 1. PL QY of solutions (excitation at 565 nm).

N_2 QY%		O_2 QY%	O_2 Hydrazine QY%	N_2 Hydrazine QY%
H_2O	DMSO	DMSO	DMSO	DMSO
15	54	45	30	47

The effect of oxygen is particularly evident in the absorption spectra of the DMSO solutions, as shown in Figure 4 on the right. In the presence of oxygen, the absorption shows a sharp reduction of the high energy peak and a consequent red shift of the maximum at around 609 nm. Treatment of the solution with hydrazine does not cause a shift in the main bands but reveals the disappearance of the 640 nm lower energy shoulder, which could be attributed to the presence of oxygen in the synthetized material due to the fact that synthesis and purification were not carried out in an inert atmosphere.

In Figure 5 the PL spectra of the water (A) and DMSO (B) solutions are reported of the four solutions whose absorption is reported in Figure 3 (right) and Figure 4 (right). When O_2 is bubbled into the solutions, a reduction of the yellow component of the PL is observed, particularly evident in the case of the DMSO solvent. By adding Hydrazine to the O_2 solution the yellow emission is partially restored. So, the Hydrazine is able to partially restore the yellow emission after it has been quenched by the O_2. By adding Hydrazine to the N_2 solutions the PL shape does not change significantly.

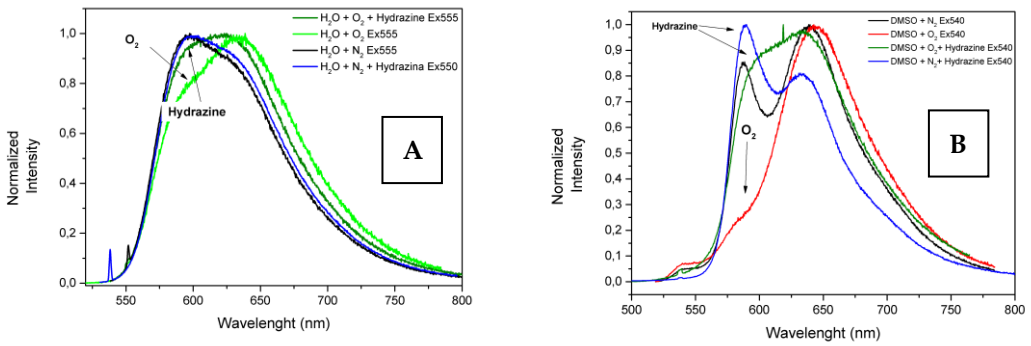

Figure 5. Emission spectrum of: [**A**] CDs in H_2O in the 4 conditions with 555 nm excitation, [**B**] of CDs in DMSO in the 4 conditions with 540 nm excitation.

When O_2 is bubbled into the DMSO + N_2 solution, analogously to the addition to Water solution, the yellow emission at 587 nm is switched-off, so each excitation in DMSO + O_2 lead to the 645 nm emission; while the absorption peaks decrease in intensity except for the one at 605 nm.

By the addition of Hydrazine to the DMSO +O_2 sample the yellow emission is pretty restored at 599 nm, while if it is added to the DMSO + N_2 solution the peak at 587 increase its intensity and red shifts at 591 nm. The lower-energy absorption component, at 605 nm, in both cases, following Hydrazine addition, disappears.

In conclusion, we have performed a photophysical analysis of water and DMSO solutions under N_2, with oxigen or hydrazine addition, in order to recognize the role of oxygen in doping the CDs. In both the solvents three components are present in the absorption and emission spectra. In DMSO an absorption component at 640 may be attributed to the presence of oxygen accompanied by a sharp reduction of the 540 nm band. The 640 nm component is present also in the brodening at lower energy of the absorpiton spectrum in water. The PL analysis shows that oxigen quenches the yellow component of the emission in in both water and DMSO. By hydrazine addition the yellow emission component is partially restored. However, the PL QY analysis in DMSO (see Tablex) shows that the addition of hydrazine induces a reduction of the overall intensity of the PL.

Author Contributions: Conceptualization, M.P. and B.M.S.; methodology, F.T., M.P. and C.B.; software, C.B. and F.M.V.; validation, F.T., M.P. and C.B.; formal analysis, F.T., C.B. and F.M.V.; investigation, F.T., C.B., M.P. and F.V.M.; resources, F.T., M.P. and C.B.; data curation, F.T., M.P. and C.B.; writing—original draft preparation, F.T.; writing—review and editing, F.T., M.P. and C.B.; visualization, F.T., M.P. and C.B.; supervision, M.P. and B.M.S.; project administration, M.P.; funding acquisition, M.P. All authors have read and agreed to the published version of the manuscript.

Funding: Please add: This research was funded by Fondazione Cariplo, circular economy for a sustainable future 2021 call, 'FENICE' (Functional carbon dots for ENhancing tomato production In a Circular Economy scheme), g.a.2021-0626 (2022-2025).

Institutional Review Board Statement:

Informed Consent Statement:

Data Availability Statement:

Conflicts of Interest:

References

1. Xu, X.; Ray, R.; Gu, Y.; Ploehn, H.J.; Gearheart, L.; Raker, K.; Scrivens, W.A. Electrophoretic Analysis and Purification of Fluorescent Single-Walled Carbon Nanotube Fragments. *J. Am. Chem. Soc.* **2004**, *126*, 12736–12737.
2. Kang, C.; Huang, Y.; Yang, H.; Yan, X.F.; Chen, Z.P. A review of carbon dots produced from biomass wastes. *Nanomaterials* **2020**, *10*, 2316.
3. Liao, J.; Yao, Y.; Lee, C.H.; Wu, Y.; Li, P. In vivo biodistribution, clearance, and biocompatibility of multiple carbon dots containing nanoparticles for biomedical application. *Pharmaceutics* **2021**, *13*, 1872.
4. Rao, L.; Zhang, Q.; Sun, B.; Wen, M.; Zhang, J.; Zhong, G.; Fu, T.; Niu, X. Multicolor Luminescent Carbon Dots: Tunable Photoluminescence, Excellent Stability, and Their Application in Light-Emitting Diodes. *Nanomaterials* **2022**, *12*, 3132.
5. Hamed, M.; Chinnam, S.; Bedair, A.; Emara, S.; Mansour, F.R. Carbon quantum dots from natural sources as sustainable probes for metal ion sensing: Preparation, characterizations and applications. *Talanta Open* **2024**, *10*, 100348.
6. Wang, B.; Cai, H.; Waterhouse GI, N.; Qu, X.; Yang, B.; Lu, S. Carbon Dots in Bioimaging, Biosensing and Therapeutics: A Comprehensive Review. *Small Sci.* **2022**, *2*, 2200012.
7. Michenzi, C.; Scaramuzzo, F.; Salvitti, C.; Pepi, F.; Troiani, A.; Chiarotto, I. Photo-Activated Carbon Dots as Catalysts in Knoevenagel Condensation: An Advance in the Synthetic Field. *Photochem* **2024**, *4*, 361–376.
8. Carioscia, A.; Cocco, E.; Casacchia, M.E.; Gentile, G.; Mamone, M.; Giorgianni, G.; Incerto, E.; Prato, M.; Pesciaioli, F.; Filippini, G.; et al. Nitrogen-Rich Carbon Dots as Effective Catalysts in the 1,4-Reduction of α,β-Unsaturated Aldehydes via Ion Pair Asymmetric Nano-Organocatalysis. *ACS Catal.* **2024**, *14*, 13429–13438.
9. Nguyen, V.-N.; Pham, H.L.; Nguyen, X.T. Recent progress in organic carbon dot-based photosensitizers for photodynamic cancer therapy. *Dye. Pigment.* **2024**, *230*, 112359.
10. Karagianni, A.; Tsierkezos, N.G.; Prato, M.; Terrones, M.; Kordatos, K.V. Application of carbon-based quantum dots in photodynamic therapy. *Carbon* **2023**, *203*, 273–310.

11. Ardini, B.; Manzoni, C.; Squeo, B.; Villafiorita-Monteleone, F.; Grassi, P.; Pasini, M.; Bollani, M.; Virgili, T. Spectral Imaging of UV-Blocking Carbon Dot-Based Coatings for Food Packaging Applications. *Coatings* **2023**, *13*, 785.
12. Lagonegro, P.; Giovanella, U.; Pasini, M. Carbon Dots as a Sustainable New Platform for Organic Light Emitting Diode. *Coatings* **2020**, *11*, 5.
13. Chen, M.; Ma, J.; Chen, C.; Ding, J.; Liu, Y.; He, H.; Liu, Q.; Hu, G.; Wu, Y.; Liu, X. Cutting-edge innovations in red carbon dots: Synthesis, perfection, and breakthroughs in optoelectronics and electrocatalysis. *Chem. Eng. J.* **2024**, *498*, 155302.
14. Qin, W.; Wang, M.; Li, Y.; Li, L.; Abbas, K.; Li, Z.; Tedesco, A.C.; Bi, H. Recent advances in red-emissive carbon dots and their biomedical applications. *Mater. Chem. Front.* **2024**, *8*, 930–955.
15. Warjurkar, K.; Panda, S.; Sharma, V. Red emissive carbon dots: A promising next-generation material with intracellular applicability. *J. Mater. Chem. B* **2023**, *11*, 8848–8865.
16. Hussain, M.M.; Khan, W.U.; Ahmed, F.; Wei, Y.; Xiong, H. Recent developments of Red/NIR carbon dots in biosensing, bioimaging, and tumor theranostics. *Chem. Eng. J.* **2023**, *465*, 143010.
17. Wang, Y.; Li, X.; Zhao, S.; Wang, B.; Song, X.; Xiao, J.; Lan, M. Synthesis strategies, luminescence mechanisms, and biomedical applications of near-infrared fluorescent carbon dots. *Coord. Chem. Rev.* **2022**, *470*, 214703.
18. Jiang, L.; Ding, H.; Xu, M.; Hu, X.; Li, S.; Zhang, M.; Zhang, Q.; Wang, Q.; Lu, S.; Tian, Y.; et al. UV–Vis–NIR Full-Range Responsive Carbon Dots with Large Multiphoton Absorption Cross Sections and Deep-Red Fluorescence at Nucleoli and In Vivo. *Small* **2020**, *16*, 2000680.
19. Liu, E.; Liang, T.; Ushakova, E.V.; Wang, B.; Zhang, B.; Zhou, H.; Xing, G.; Wang, C.; Tang, Z.; Qu, S.; et al. Enhanced Near-Infrared Emission from Carbon Dots by Surface Deprotonation. *J. Phys. Chem. Lett.* **2021**, *12*, 604–611.
20. Zhang, H.; Wang, G.; Zhang, Z.; Lei, J.H.; Liu, T.-M.; Xing, G.; Deng, C.-X.; Tang, Z.; Qu, S. One step synthesis of efficient red emissive carbon dots and their bovine serum albumin composites with enhanced multi-photon fluorescence for in vivo bioimaging. *Light Sci. Appl.* **2022**, *11*, 113.
21. Shi, W.; Yao, Q.; Qu, S.; Chen, H.; Zhang, T.; Chen, L. Micron-thick highly conductive PEDOT films synthesized via self-inhibited polymerization: Roles of anions. *NPG Asia Mater.* **2017**, *9*, e405.
22. Yemata, T.A.; Zheng, Y.; Kyaw AK, K.; Wang, X.; Song, J.; Chin, W.S.; Xu, J. Modulation of the doping level of PEDOT:PSS film by treatment with hydrazine to improve the Seebeck coefficient. *RSC Adv.* **2020**, *10*, 1786–1792.
23. Tao, S.; Zhu, S.; Feng, T.; Xia, C.; Song, Y.; Yang, B. The polymeric characteristics and photoluminescence mechanism in polymer carbon dots: A review. *Mater. Today Chem.* **2017**, *6*, 13–25.
24. Xia, C.; Zhu, S.; Feng, T.; Yang, M.; Yang, B. Evolution and Synthesis of Carbon Dots: From Carbon Dots to Carbonized Polymer Dots. *Adv. Sci.* **2019**, *6*, 1901316.
25. Mondal, M.; Pramanik, S. A mechanism for excitation-dependent emission from carbon nanodots. *Mater. Lett. X* **2023**, *18*, 100195.
26. Liu, E.; Liang, T.; Ushakova, E.V.; Wang, B.; Zhang, B.; Zhou, H.; Xing, G.; Wang, C.; Tang, Z.; Qu, S.; et al. Enhanced Near-Infrared Emission from Carbon Dots by Surface Deprotonation. *J. Phys. Chem. Lett.* **2021**, *12*, 604–611.